PHYSICS OF FLUIDS VOLUME 16, NUMBER 11 NOVEMBER 2004

A new large-eddy simulation near-wall treatment

M. Iovieno
Dipartimento di Ingegneria Aeronautica e Spaziale, Politecnico di Torino, Corso Duca degli Abruzzi 24, 10129 Torino, Italy

G. Passoni
Dipartimento di Ingegneria Idraulica, Politecnico di Milano, Ambientale, Rilevamento Piazza Leonardo da Vinci 32, 20133 Milano, Italy

D. Tordella[a)]
Dipartimento di Ingegneria Aeronautica e Spaziale, Politecnico di Torino, Corso Duca degli Abruzzi 24, 10129 Torino, Italy

(Received 24 February 2004; accepted 4 June 2004; published online 5 October 2004)

Two different types of instantaneous wall boundary conditions have been proposed for resolved large scale simulations that extend inside the viscous sublayer. These conditions transfer the physical no-slip and impermeability/permeability information, which can only be rigorously applied to the unfiltered variables, to the filtered variables. The first condition is universal, while the second one specifies the wall stress and relevant distribution and can be used to treat inverse flow problems. The filter scale close to the wall is a function which varies according to its position and thus the problem of the noncommutation of the filter and differentiation operators arises. Used together with the explicit noncommutation procedure by Iovieno and Tordella, these boundary conditions constitute a wall treatment which could improve the use of the large-eddy methodology in relation to aspects that are independent of the modeling of the subgrid scale motion. When applied in the test case of the plane periodic channel, intentionally using the most crude subgrid scale model (Smagorinsky, with no dynamic procedure or wall damping function) to prove its efficacy, the proposed near-wall treatment yielded resolved large-eddy simulations which compare well with both direct numerical simulations and with experimental data. The effects of the Reynolds number on the structure of the flow are retained. Distributions of the noncommutation error on the turbulent solution are also reported. © *2004 American Institute of Physics*. [DOI: 10.1063/1.1783371]

I. INTRODUCTION

The large-eddy simulation (LES) method is probably going to be one of the most frequently used tools to predict the behavior of turbulent flows for many different physical and engineering applications. Among these applications, wall flows constitute a separate class, due to the peculiarities of the near-wall dynamics that are related to important applications in geophysics, hydrodynamics, and gasdynamics. The turbulence near the wall is very unhomogeneous and not in equilibrium. The diffusive vorticity generation is coupled and is of the same order as the unsteadiness and nonlinearity. Such a complex situation is not easily synthesized in a model, because, close to the wall, the categories on which the turbulence modeling of homogeneous or nearly homogeneous flows relies are not valid, the conceptual separation between the large and small scales is not possible, and the asymptotics similarity is not observed in practical problems. It is crucial for physicists and engineers, who nevertheless must produce approximate but reliable forecasts to improve the use of the method as much as possible independently of the physical features of the subgrid scale model that is adopted. For this purpose it is important to consider the following: (1) the transfer of the wall physical conditions, which can only be rigorously applied to the unfiltered variables, to the filtered variables and (2) the noncommutation property loss between the filter and differentiation operations, which affects the simulation of unhomogeneous fields, such as the wall flows, in which the filter scale varies greatly according to the position $[\boldsymbol{\delta}=\boldsymbol{\delta}(x_i)]$.[1–5] In this situation, the governing equations change structure, because a noncommutation term must be introduced in correspondence to each spatial differential term. The change in the filtered governing equations introduces variations to their numerical solution.

For high Reynolds number flows, the problem of the boundary conditions for the filtered field can be treated by adopting one of the classical approximated conditions that relies on the introduction of special wall models, which represent the inner layer dynamics [usually in a Reynolds-averaged sense, see the review by Piomelli and Balaras, Sec. 2 (Ref. 6)], and by putting the first grid point used by the large-eddy simulation inside the logarithmic layer (see Ref. 7, the wall-stress models by Schumann[8] and Piomelli *et al.*,[9] the two-layer models by Balaras *et al.*,[10] the detached eddy simulation approach by Baggett[11] and Nikitin *et al.*[12]). These models were conceived to avoid the prohibitively expensive computational cost of resolving the wall layer in high Reynolds number environmental and engineering applications. However, at a fundamental level, with regard to the LES

a)Author to whom correspondence should be addressed. Telephone: 0039 011 564 6812; fax: 0039 011 564 6899; electronic mail: daniela.tordella@polito.it

methodology, and to resolve the near-wall dynamics, it is also acceptable to place grid points inside the viscous sublayer.

The boundary conditions for the filtered variables should be different from those that are canonical for the unfiltered variables, i.e., the no-slip and impermeability conditions $u_i = 0$ at the wall. First, the filtering operation (e.g., the volume average) is ill defined for grid points placed on the wall because, in this case, the filter width extends beyond the wall boundary (i.e., outside the flow domain); second, a filtering volume in contact with the wall, but entirely merged within the domain, will give averaged velocities that are different from zero and which are placed in the dynamical center of the average volume which will always be located at a finite distance from the wall.

On the other hand, the alternative option of the grid refinement (i.e., the filter width that goes to zero as the wall is approached) is not clearly defined. In this case in fact it is not possible to automatically determine where the shift from LES to DNS takes place. This shift would necessitate the change of the evolution equations from the filtered NS version (LES) to the unfiltered NS (DNS). Since this change is not carried out, which would inevitably imply the introduction of a domain decomposition, the simulation cannot be considered as being based on a consistent problem form. Furthermore, even in the hypothesis of having consistently split the domain to carry out the hybrid LES-DNS, it would mean adopting a time step which must fit the DNS requirements close to the wall. The temporal integration scale for the DNS is faster than that required by the LES, but since it is not possible, advancing on time, to differentiate the temporal steps into different regions of the computational domain, the DNS requirement would take precedence over the LES one, and this is not convenient.

It is here proposed to shift the boundary conditions for the filtered field onto a surface that lies on a first level of grid points and is parallel to the wall, at a distance of the same order as the viscous length. The transfer of the information that is relevant to the physical properties of the wall is accomplished by considering a series expansion in $\boldsymbol{\delta}$ for the filtered variable, at the first layer of points. If associated to a Taylor expansion of the unfiltered variable at the wall, this yields a first kind of condition that is universal in character. If the $\boldsymbol{\delta}$ expansion is instead related to a Mac Laurin expansion of the unfiltered variable at the wall, a second kind of boundary condition is obtained which is suitable to impose a known distribution of wall stresses, as normally asked in the context of inverse mathematical problems. The boundary condition formulations are described in Sec. II. The related *a priori* tests,[13] which showed a correlation with DNS data[14,15] as high as 0.97 for a boundary shift of five wall units, are described in Sec. II A.

As previously explained, the other feature that has been implemented in the simulations is the noncommutation procedure.[1] This is based on an approximation of the different noncommutation terms in the governing equations as functions of the $\boldsymbol{\delta}$ gradient and of the $\boldsymbol{\delta}$ derivatives of the filtered variables. The anisotropic noncommutation approximating terms, of the fourth order of accuracy in the filter scale, are obtained using series expansion in $\boldsymbol{\delta}$ of approximations based on finite differences and introducing two successive levels of filtering. A brief outline of this procedure is given in Sec. III. The distribution of the noncommutation errors on the Reynolds stresses is given in Sec. IV.

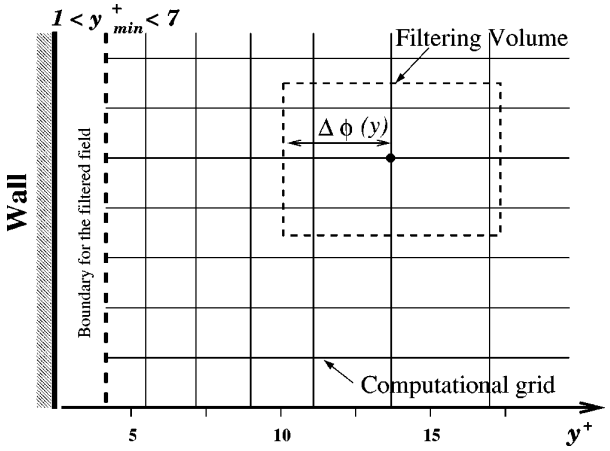

FIG. 1. A schematic view of the shifted boundary conditions, the filter, and the grid.

The results that were obtained when using the present wall treatment applied to the LES of the channel flow and obtained by utilizing the most crude SGS model (Smagorinsky, with no dynamic procedure or wall damping function) are discussed in Sec. IV. The simulations compare well with the direct numerical simulations[14,15] and with laboratory observations.[16–18] The simulations show the correct Reynolds number dependency. Given this, much greater progress can be expected if the dynamic procedure[19,20] and models which allow for significant nonlocal and nonequilibrium effects are used.[21–24] The concluding remarks are given in Sec. V.

II. NEAR-WALL TREATMENT

A. Wall conditions for the filtered variables

The shifting of the boundary conditions for the filtered field on a surface that lies beside the wall at a distance $\underline{y}$ of the same order as the viscous length ℓ_τ [$\underline{y} = O(\ell_\tau) = O(\delta_{\min})$], see Fig. 1, is here proposed. The first level of the grid points should in turn be positioned on the shifted boundary. This shift offers a twofold advantage—first, the dependent variables are correctly determined, as it is possible to set a local volume of integration which does not cut the physical boundary; and second, since the shifted boundary is close to the wall, it is possible to transfer the physical information that corresponds to the no-slip and impermeability/permeability conditions to the shifted condition through a series expansion. An expansion in series of $\boldsymbol{\delta}$ of the filtered variable can in fact be associated, at the first layer of points, to a Taylor or a Mac Laurin expansion of the unfiltered variable at the wall, where the filter length reaches the minimum value normal to the wall $\delta_{\min}$. While using this boundary formulation, one is aiming at simulating the inner viscous layer in the region $y^+ < 50$, which requires $\delta_{\min} = \underline{y} \sim 1$–5.

Let us consider the class of integration volumes

$$V_{\boldsymbol{\delta}}=\left\{\boldsymbol{\xi}\in\mathbb{R}^3:\left\|\left(\frac{\eta_1}{\delta_1},\frac{\eta_2}{\delta_2},\frac{\eta_3}{\delta_3}\right)\right\|<1\right\}, \tag{1}$$

where $\boldsymbol{\delta}(\mathbf{x})=(\delta_1(\mathbf{x}),\delta_2(\mathbf{x}),\delta_3(\mathbf{x}))$ and the transformation $\eta_j=\delta_j\xi_j$ [with $\det(\partial\eta_i/\partial\xi_k)=\delta_1\delta_2\delta_3$ and where no summation is implied] has been introduced. Let us consider the average operation for the variable $f(\mathbf{x})=f(x_j+\delta_j\xi_j)$:

$$\langle f\rangle_{\boldsymbol{\delta}}=\frac{1}{V_{\boldsymbol{\delta}}}\int_{V_{\boldsymbol{\delta}}}f(\mathbf{x}+\boldsymbol{\eta})d\boldsymbol{\eta}=\frac{1}{V_{\mathbf{1}}}\int_{V_{\mathbf{1}}}f(x_j+\delta_j\xi_j)d\boldsymbol{\xi}, \tag{2}$$

where $\mathbf{1}=(1,1,1)$ and $V_{\mathbf{1}}=V_{\boldsymbol{\delta}}/\delta_1\delta_2\delta_3$.

For the sake of simplicity, let us now consider the case of a flat wall flow. Here the filter can be opportunely represented by the widely used notation $\boldsymbol{\delta}(\mathbf{x})=(\Delta x,\varphi(y)\Delta y,\Delta z)$ with constants Δx, Δy, and Δz and where y is the coordinate normal to the wall. The $\boldsymbol{\delta}$ expansion for a general variable f, after setting $\delta(\underline{y})\cong\delta_{\min}=\varphi_{\min}\Delta$, yields

$$\langle f\rangle(\underline{y})=f(\underline{y})+L[f]\delta_{\min}^2+O\left(\delta_{\min}^4\right), \tag{3}$$

where

$$L[\cdot]=\tfrac{1}{2}a\tilde{\nabla}^2,\quad \tilde{\nabla}=\partial_{y^2}^2+\left(\frac{\Delta x}{\delta_{\min}}\right)^2\partial_{x^2}^2+\left(\frac{\Delta_z}{\delta_{\min}}\right)^2\partial_{z^2}^2, \tag{4}$$

$$a=\frac{1}{V_1}\int_{V_1}\xi_i^2d\boldsymbol{\xi}, \tag{5}$$

and where it should be recalled that, due to (1) and (2), the coefficients of the odd powers of $\delta_{\min}$ are zero. By applying the operator L to (3) one obtains

$$L[\langle f\rangle]=L[f]+L[\delta_{\min}^2L[f]]+O\left(\delta_{\min}^4\right)=L[f]+O\left(\delta_{\min}^2\right). \tag{6}$$

As a consequence, (3) can be written as

$$f(\underline{y})=\langle f\rangle(\underline{y})-\delta_{\min}^2L[\langle f\rangle]+O\left(\delta_{\min}^4\right). \tag{7}$$

In turn, to transfer the no-slip and impermeability information, which applies at $y=0$, let us consider the Taylor expansion along the normal to the wall,

$$f(0)=f(\underline{y})-\underline{y}\partial_yf(\underline{y})+\frac{\underline{y}^2}{2}\partial_yf(\underline{y})+O(\underline{y}^3). \tag{8}$$

Since relation (6) can be generalized as

$$\frac{d^m}{dx^m}f(x_j)=\frac{d^m}{dx^m}\langle f\rangle(x_j)+O(\delta^2),\quad m=1,2,\ldots, \tag{9}$$

expansion (8) can be written as

$$f(\underline{y})=f(0)+\underline{y}\partial_y\langle f\rangle-\frac{\underline{y}^2}{2}\partial_y^2\langle f\rangle+O\left(\delta_{\min}^3\right). \tag{10}$$

By equating (7) and (10), while recalling definition (4), and truncating the third-order terms, a new boundary condition is obtained at $y=\underline{y}$,

$$\langle f\rangle=f(0)+\underline{y}\partial_y\langle f\rangle+\frac{1}{2}a\tilde{\nabla}^2[\langle f\rangle]\delta_{\min}^2-\frac{\underline{y}^2}{2}\partial_y^2\langle f\rangle, \tag{11}$$

where the filtered variable at each instant depends explicitly on the position $\underline{y}$, the values of its first and second derivatives, and the wall value of the unfiltered variable, which introduces the physical information. This condition—which in the following is called condition I—is an instantaneous condition and it is universal because it can be applied to any kind of wall boundary. One should note that, according to the theory established by Kreiss[25] for Dirichlet differential problems discretized with a finite-difference scheme with order $O(\delta^p)$ at inner points and $O(\delta^{p-1})$ at points close to the boundary, the error of the discrete solution is $O(\delta^p)$ throughout. Therefore, with such a boundary condition formulation and truncating the terms of order $O(\delta^3)$, the fourth order of accuracy reached for the approximation of the noncommutation term proposed by Iovieno and Tordella[1] can be expected to be preserved. In the present simulation, the y derivatives of the filtered variables at $y=\underline{y}$ have been calculated using one-sided discrete operators.

Another similar type of boundary condition can be written by equating (7) to the Mac Laurin series $f(\underline{y})=f(0)+\underline{y}\partial_yf\,|_{y=0}+(\underline{y}^2/2)\partial_y^2f\,|_{y=0}+O(\underline{y}^3)$, which gives the condition

$$\langle f\rangle=f(0)+\underline{y}\partial_yf\,|_{y=0}+\frac{\underline{y}^2}{2}\partial_y^2f\,|_{y=0}+\frac{a}{2}\delta_{\min}^2\tilde{\nabla}^2[\langle f\rangle]. \tag{12}$$

In the case of a steady (in the mean) turbulent flow it is possible, with this formulation, to transfer the information relevant to the time average of the wall shear stress distribution and its derivative to the filtered field. Condition (12)—which in the following is called condition II—is an instantaneous condition. However, it is physically reasonable to insert the time averaged values of the wall stress only in the case of flows which are steady in the mean, as is the case of the example that we have considered in this paper. However, this is not the only possibility. In fact, if detailed information on the temporal and spatial variation of the wall stress are available, it would in fact be better to insert them into infield condition II. The innovative and original character of condition II is that it allows the flow to be fed with different wall information, which, apart from the pure no-slip condition, also includes information on the time and space fluctuations, or possible evolutions of the wall stress along the wall. All this can be gathered in one single condition. This is feasible because, having placed the condition relatively close to the wall—at a distance of almost one viscous length—one can use a Mac Laurin series expansion to transfer the physical information at the wall to the infield condition. In other words, a convenient situation is obtained: instead of using the physical boundary—the wall—where only one boundary condition (bc) can be placed for each variable (on the variable itself or on one of its derivatives in the direction normal to the wall), one can give a plurality of information concerning the values of the variables and of their relevant wall derivatives to the field, with just one condition and without overconstraining the flow.

A solution accuracy of the fourth order could also be expected when using this boundary condition (see the previous comments). It must be noticed that, with this kind of formulation, the shear stress distribution along the wall can be imposed to the field, as can the related characteristics such as the intensity of the wall roughness. In this case, this boundary condition can be applied to inverse mathematical problems.

B. *A priori* test on the approximate boundary conditions

The correlation between the filtered values that are obtained by the present shifted boundary conditions and the filtered values that are obtained by a direct numerical simulation can be defined, as a function of the distance of the shifted boundary from the wall, as

$$C=\overline{(\langle u_i\rangle_{DNS}-\overline{\langle u_i\rangle_{DNS}})(\langle u_i\rangle-\overline{\langle u_i\rangle})}/\sqrt{\mathrm{var}(\langle u_i\rangle_{DNS})\mathrm{var}(\langle u_i\rangle)}\,, \tag{13}$$

where $\langle u_i\rangle_{DNS}$ are the filtered data from the direct simulation data base (Passoni *et al.*[15]), $\langle u_i\rangle$ have been computed from (11) and (12) by introducing the filtered direct simulation data into the right-hand side, the overbar means the average over the surface parallel to the wall, and var is the variance. For $\mathrm{Re}_\tau=180$ (the Reynolds number for which a wide set of instantaneous fields was available) Fig. 2 shows that both boundary conditions I and II yield a correlation C which is over 0.97 for the three velocity components up to a distance of five wall units and goes down to 0.8, 0.88, 0.7 for $\langle u\rangle,\langle v\rangle,\langle w\rangle$, respectively, at seven wall units.

C. Noncommutation treatment

The noncommutation procedure and the new wall condition models together constitute the new treatment for wall turbulence that is here proposed. The main applications that require a highly variable filtering in LES are wall flows. They must be represented through (a) accessory conditions that are consistent with the LES methodology, on the one hand, and (b), on the other hand, a possibly explicit noncommutation procedure. As explained in the Introduction, apart from the matter relevant to the quality of either dynamical or not subgrid model, the no-slip condition associated to the use of a filter width which goes to zero as the wall is approached is not a fully consistent treatment for large-eddy simulations of near-wall turbulence.

A brief description of the noncommutation procedure is given in the following. When $\boldsymbol{\delta}$, the linear scale of filtering, is not uniform in the flow domain, the averaging and differentiation operations no longer commute. This leads to inhomogeneous terms in the motion equations that act as source terms whose intensity depends on the gradient of the filter scale $\boldsymbol{\delta}$ and which, if neglected, induce a systematic error throughout the solution. One kind of noncommutation term for each differential term is present in the governing equations. By introducing the subgrid turbulent stresses $R_{ij}^{(\boldsymbol{\delta})}=\langle u_i\rangle_{\boldsymbol{\delta}}\langle u_j\rangle_{\boldsymbol{\delta}}-\langle u_iu_j\rangle_{\boldsymbol{\delta}}$ and the noncommutation terms $\mathcal{C}_i'$,$\mathcal{C}_{ii}''$, for the first and second derivatives, as discussed by

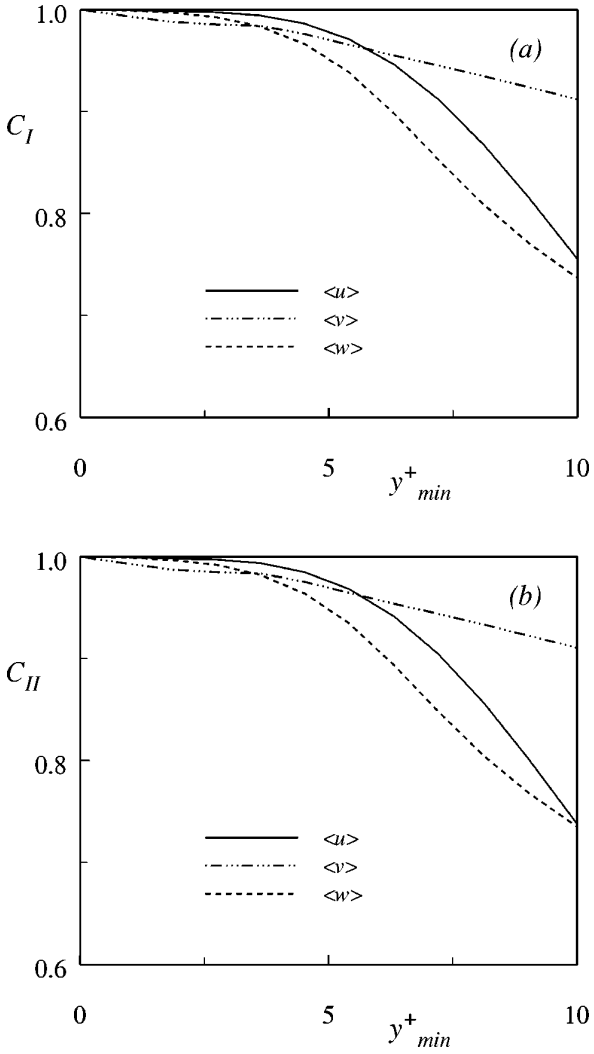

FIG. 2. An *a priori* test on the approximate boundary conditions: correlation level as a function of the distance $y_{\min}=\underline{y}$ of the shifted boundary from the wall. Top panel condition I, Eq. (11); bottom panel condition II, Eq. (12).

Iovieno and Tordella[1] (see there, Sec. II for the isotropic filter configuration and the Appendix for the general anisotropic and the wall-bounded flow configurations) the averaged governing equations can be written as

$$\partial_i\langle u_i\rangle_{\boldsymbol{\delta}}=-\mathcal{C}_i'(\langle u_i\rangle_{\boldsymbol{\delta}})\,, \tag{14}$$

$$\partial_t\langle u_i\rangle_{\boldsymbol{\delta}}+\partial_j(\langle u_i\rangle_{\boldsymbol{\delta}}\langle u_j\rangle_{\boldsymbol{\delta}})+\partial_i\langle p\rangle_{\boldsymbol{\delta}}-\nu\partial_{jj}^2\langle u_i\rangle_{\boldsymbol{\delta}}-\partial_jR_{ij}^{(\boldsymbol{\delta})}$$
$$=-\mathcal{C}_j'(\langle u_i\rangle_{\boldsymbol{\delta}}\langle u_j\rangle_{\boldsymbol{\delta}})-\mathcal{C}_i'(\langle p\rangle_{\boldsymbol{\delta}})+\nu\mathcal{C}_{jj}''(\langle u_i\rangle_{\boldsymbol{\delta}})+\mathcal{C}_j'(R_{ij}^{(\boldsymbol{\delta})})\,. \tag{15}$$

The present procedure approximates the noncommutation terms on the right-hand side of (14) and (15) by means of series expansion in $\boldsymbol{\delta}$ of finite difference approximations of the space derivatives and by introducing a successive level of filtering. An accuracy of the fourth order is reached with respect to $\boldsymbol{\delta}$.

Let us recall that the anisotropic noncommutation term of the first derivative $\mathcal{C}_i'$, defined by

$$C_i'(\langle f\rangle_{\boldsymbol{\delta}}) = \left\langle \frac{\partial f}{\partial x_i} \right\rangle_{\boldsymbol{\delta}} - \frac{\partial}{\partial x_i}\langle f\rangle_{\boldsymbol{\delta}}, \tag{16}$$

can be represented as the sum of the products of the filter space derivatives and the filter derivatives of the filtered variable:

$$C_i'(\langle f\rangle_{\boldsymbol{\delta}}) = -\sum_{j=1}^{3} \frac{\partial \delta_j}{\partial x_i}\frac{\partial}{\partial \delta_j}\langle f\rangle_{\boldsymbol{\delta}}. \tag{17}$$

For flow fields where the domain grid needs to be stretched along only one direction, say y, and whose typical examples are two-dimensional wall-bounded flows, the last representation yields very simple approximation formulas. By adopting the notation $\boldsymbol{\delta}(\mathbf{x}) = (\Delta x, \varphi(y)\Delta y, \Delta z)$ with constants $\Delta x, \Delta y$, and Δz, the anisotropic approximation for the first derivative noncommutation term results

$$\tilde{C}_y'(\langle f\rangle_{\boldsymbol{\delta}}) = -\frac{\partial \varphi}{\partial y}\frac{1}{2\varphi(y)}\left(\langle\langle f\rangle_{\boldsymbol{\delta}}\rangle_{2\varphi(y)\Delta y} - \langle f\rangle_{\boldsymbol{\delta}}\right). \tag{18}$$

Similarly, the anisotropic noncommutation term of the second derivatives, being defined by

$$C_{ii}''(\langle f\rangle_{\boldsymbol{\delta}}) = \left\langle \frac{\partial_2 f}{\partial x_i^2} \right\rangle_{\boldsymbol{\delta}} - \frac{\partial^2}{\partial x_i^2}\langle f\rangle_{\boldsymbol{\delta}}, \tag{19}$$

can be written as

$$C_{ii}''(\langle f\rangle_{\boldsymbol{\delta}}) = -\sum_{j=1}^{3} \frac{\partial^2 \delta_j}{\partial x_i^2}\frac{\partial}{\partial \delta_j}\langle f\rangle_{\boldsymbol{\delta}} - 2\sum_{j=1}^{3} \frac{\partial \delta_j}{\partial x_i}\left(\frac{\partial^2}{\partial \delta_j \partial x_i}\langle f\rangle_{\boldsymbol{\delta}}\right) - \sum_{j,k=1}^{3}\left(\frac{\partial \delta_j}{\partial x_i}\frac{\partial \delta_k}{\partial x_i}\right)\frac{\partial^2}{\partial \delta_j \partial \delta_k}\langle f\rangle_{\boldsymbol{\delta}}. \tag{20}$$

Again, in analogy with what has been done for the first derivatives the following approximation is obtained:

$$\tilde{C}_{yy}''(\langle f\rangle_{\boldsymbol{\delta}}) = -\frac{\varphi\partial_y^2\varphi + (\partial_y\varphi)^2}{2\varphi^2(y)}\left[\langle\langle f\rangle_{\boldsymbol{\delta}}\rangle_{2\varphi(y)\Delta y} - \langle f\rangle_{\boldsymbol{\delta}}\right] - \frac{\partial_y\varphi}{\varphi(y)}\left[\langle\partial_y\langle f\rangle_{\boldsymbol{\delta}}\rangle_{2\varphi(y)\Delta y} - \partial_y\langle f\rangle_{\boldsymbol{\delta}}\right]. \tag{21}$$

It should be remarked that this procedure operates in the physical space and does not rely on the use of a mapping function of the nonuniform grid. The present noncommutation procedure is based on the use of the volume averages; however it can be observed that it remains valid in the case where a more general kind of filtering is adopted. In the general situation, the introduction of a weight function $g(\boldsymbol{\xi})$ only modifies the numerical coefficients [such as the coefficient a in (5)] of the series expansion in $\boldsymbol{\delta}$,[1] which are only functions of the filtering domain and of the weight function, if present. The noncommutation terms and its approximations remain unchanged, provided the weight function has a compact support. The compactness of the support allows the filtered variables to be fully supported inside the physical domain. As a consequence, noncommutation terms associated to a finite or semi-infinite computational domain in the filtered equations are not present.[4] The filtered equations (14) and (15) are invariant under Galilean transformations.

III. DATA ANALYSIS RATIONALE

The large-scale flow field is obtained by directly integrating the filtered, three-dimensional, time dependent Navier–Stokes equations. The simulation quality depends to a great extent on the model that is used to represent the small-scale field motions. However, the present study concerns features of the LES method which are intrinsically independent of the subgrid scale model that is used in the simulation. Furthermore, if, on the one hand, the interference of the efficiency of the subgrid scale turbulence model with the performance yielded by the use of the new boundary conditions and noncommutation procedure must be avoided, on the other hand, it is not evident, at the state of the art, which is the best near-wall SGS model to use. Given this, it was eventually decided to accept a systematic error in the simulation prediction close to the wall by implementing the simplest and perhaps least appropriate SGS model, which is the Smagorinsky model used without the dynamic procedure or a wall damping function. Thus, *a priori* foreseeing a poor agreement in a portion of the viscous sublayer (let us call it the SGS model systematic error, SGSmSE), the behavior of the present large-scale simulations is sought and compared with direct numerical computations and laboratory observations.

The governing equations (14) and (15) were integrated in time using a hybrid pseudospectral fourth-order finite difference method. An explicit third-order Runge–Kutta scheme was used. According to the concept of minimal flow unit in near-wall turbulence by Jimenez and Moin,[26] the dimensions of the computational domain were chosen as $2\pi h, 2h, \pi h$, where h is the channel mid height, in the streamwise, crosswise, and spanwise directions, respectively. Periodic boundary conditions were applied in the streamwise and spanwise directions. Conditions I (11) and II (12) were applied as approximate wall conditions. The mesh was made up of $48\times65\times32$ points for $\mathrm{Re}_\tau=180$ and $84\times129\times56$ points for $\mathrm{Re}_\tau=590$. In the present channel flow simulations, while using type II boundary conditions, time averaged values were assigned for the wall stress, the nondimensional constant pressure gradient, and for $\partial_y\tau|_0$, zero.

Results

A few results concerning the near-wall dynamics of the turbulent channel flow are compared in this section with direct simulation results (Moser *et al.*,[14] Passoni *et al.*[15]) and experimental laboratory results (Eckelmann,[16] Kastrinakis and Eckelmann,[17] Wei and Willmarth[18]) at $\mathrm{Re}_\tau=180$ and 590. The boundary conditions are shifted to $y^+=2$ and 5.

The comparison is based on the mean velocity distribution, the distributions of the Reynolds stresses, the resolvable turbulence intensity, and the ratio between the kinetic energy production and the dissipation.

It should be noted that in most subgrid-scale stress models, in particular in the most commonly used model by Smagorinsky, the eddy viscosity is determined by assuming that

the small scales are in equilibrium. In the presence of mean shear—and thus close to solid boundaries—this position causes excessive damping of the large-scale fluctuations and viscous stresses and amplification of the subgrid-scale stresses. Modifications were made to the Smagorinsky model in the near-wall region of the plane channels to force the subgrid-scale stresses to vanish at the solid boundary through damping functions (Moin and Kim,[27] Piomelli *et al.*[9]) or a dynamic procedure (Germano *et al.*,[19] Germano[20]) was introduced. The present simulations that are carried out deliberately neglecting the use of either the dynamic procedure or damping function, due to the SGSmSE, experience a slight lower slope in the first part of the viscous sublayer, as far as the mean velocity, viscous stress, and Reynolds stress distributions are concerned.

Figure 3 shows the mean streamwise velocity across the channel. Part (a) concerns $\mathrm{Re}_\tau=180$. For such a low value of the flow control parameter, the agreement that can be obtained for a boundary condition shift of five wall units is still good (for both conditions I and II the relative local error with respect to the direct numerical computation is lower than 5%, a value which goes down to 2% for a shift of two wall units). If the control parameter is raised to $\mathrm{Re}_\tau=590$, the foreseen systematic error shows. In Fig. 3(b), the mean velocity distribution starts at $y^+=2$ with a good estimate of the local speed for both conditions I and II, but with a lower slope, which, however, the noncommutation procedure is able to compensate in such a way that, beyond $y^+\sim 40$, the slope is very close to that of the direct simulation data. A local inaccuracy of 5% is eventually obtained in the central part of the flow. An integral accuracy of 8.7%, measured by the norm L_2, is obtained in the first 100 y^+. However, for example, using condition II, this uncertainty falls to 1.9% if the SGS model is roughly optimized using the Van Driest damping function.

Figures 4 and 5 explain the behavior of the Reynolds stress $\langle \overline{uv} \rangle$ for the two values of the control parameter that were considered here. If the systematic error of the model (SGSmSE, see the shaded area in the figures) is excluded, the present near-wall treatment shows a very good agreement with the reference data. In particular, the Reynolds stress that is obtained when using condition I is very close to the DNS stress, while that obtained using condition II is very close to the set of laser-Doppler anemometer results that were obtained by Wei and Willmarth.[18] It should be pointed out that the two models are different: model I is universal, i.e., it can be used in any situation, while model II is more suitable to feed the flow with a great deal of information concerning the values of the variables and their derivatives at the wall, which can also include information on the time and space fluctuations, or possible evolutions along the wall, but this information should be available. Moreover, if this information is available, condition II, with only one equation and without overconstraining the field, allows the flow to yield not only the value of the variable or of one of its y derivatives, as is usually the case when the boundary is put on the wall itself, but all these values together. In the particular situation presented here, a first reason for the different behavior between type I and II boundary conditions is the way

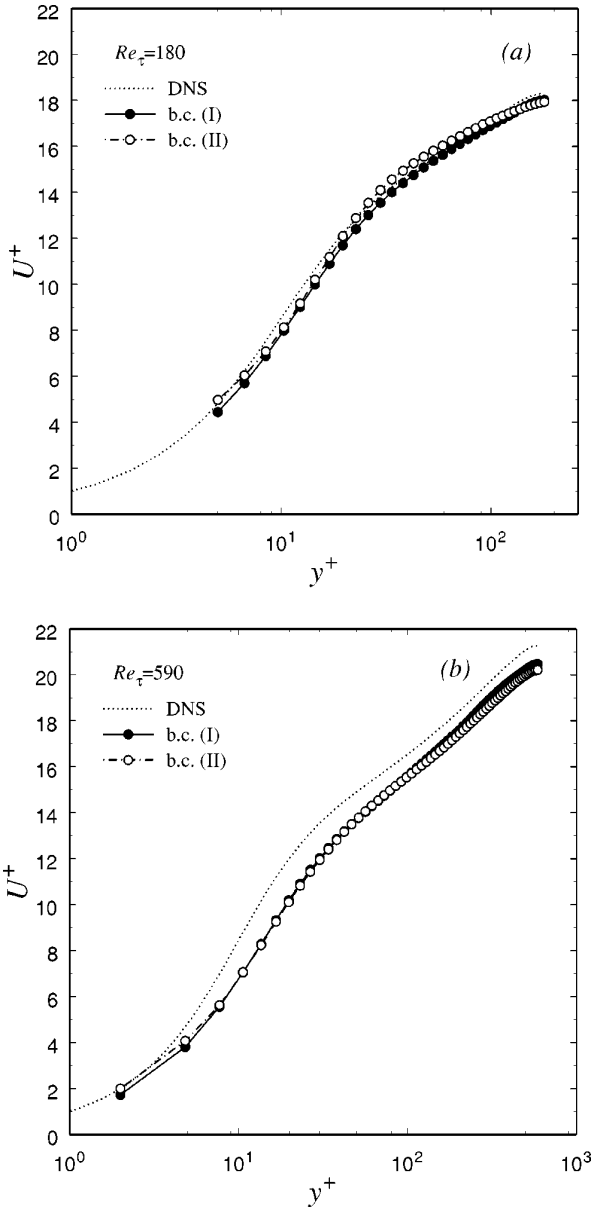

FIG. 3. The mean velocity distribution across the channel. In (b), $\mathrm{Re}_\tau=590$, the SGSmSE which induces the discrepancy in the derivative at the shifted boundary appears. However, it is also apparent that the present wall treatment recovers this error. Beyond $y^+\sim 20$ the LES and DNS are in fact parallel. This systematic error will not be present if improved SGS models, see Sec. I, are used.

in which we have used condition II, that is, the mimimal (crudest) information level allowed by this model condition. By putting the time averaged values of the first and second y derivatives of the mean velocity into bc II (i.e., for the wall stress, the nondimensional constant pressure gradient, and for $\partial_y \tau|_0$, zero), we have in fact almost frozen the time fluctuations at $\underline{y}$, that is, where we apply the bc. This imposes a local underestimation of the time fluctuations of $\langle u_i \rangle$ in the surroundings of $\underline{y}$ as compared to what happens when using the universal condition I. Another reason is that the local underestimation of the fluctuations at the field position where

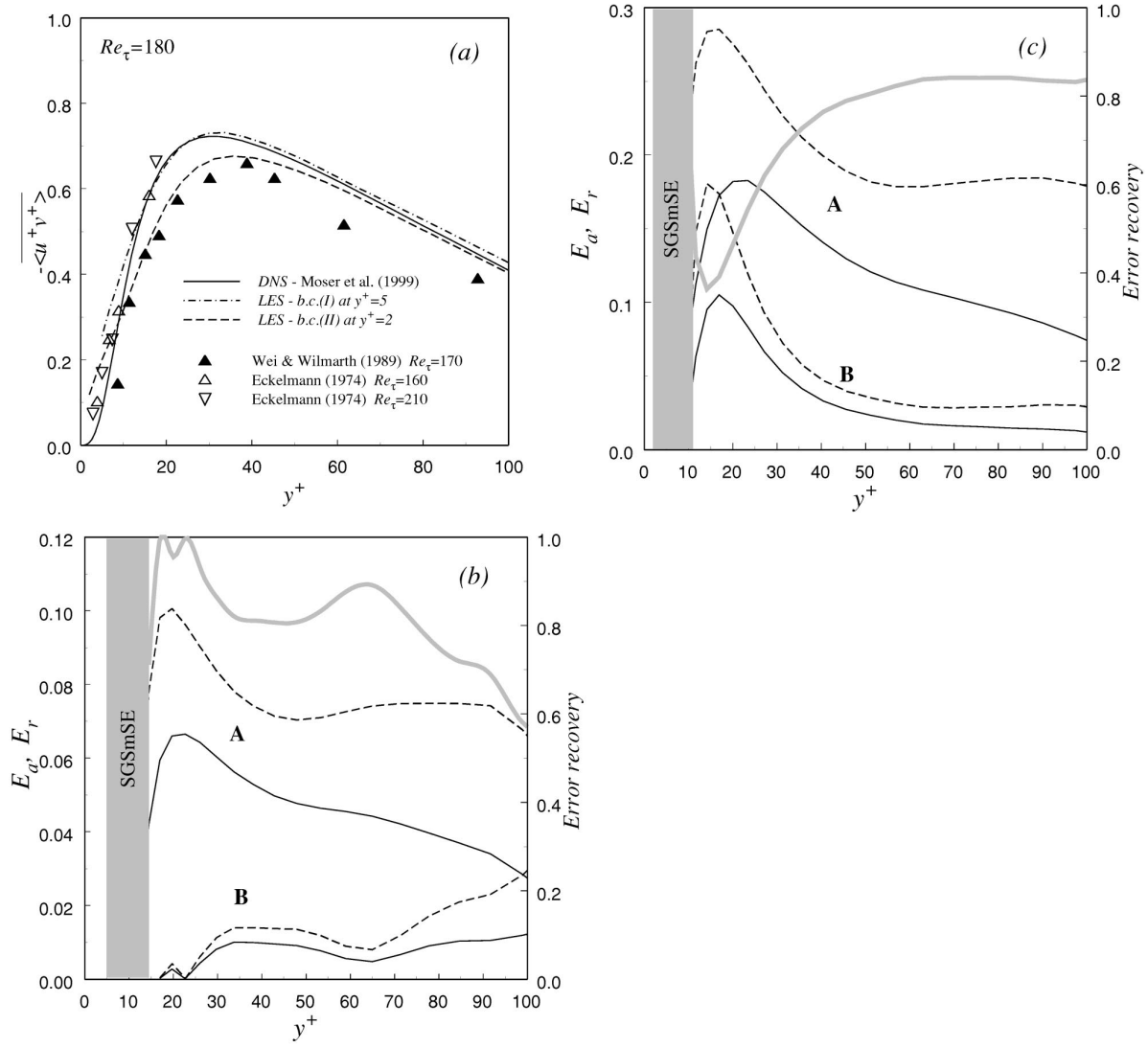

FIG. 4. $Re_\tau=180$, Reynolds stress distribution across the channel. Absolute $E_a=\langle u^+v^+\rangle-\langle u^+v^+\rangle_{DNS}$ (—) and relative $E_r=[\langle u^+v^+\rangle-\langle u^+v^+\rangle_{DNS}/\langle u^+v^+\rangle_{DNS}]$ ×(----) error distributions on the Reynolds stress distributions for boundary conditions I (b) and II (c)—**A**, without the commutation correction, **B**, with the commutation correction. Gray continuous curve: error recovery $[E_a(\mathbf{A})-E_a(\mathbf{B})]/E_a(\mathbf{A})$. Shaded area: unreliable error distributions due to the systematic error of the SGS model.

the bc is placed, in turn, induces a lowering of the intensity of the subgrid terms in the filtered equations in the viscous sublayer, compared to what happens when using bc I, and this inevitably causes a discrepancy between solutions I and II.

Parts (b) and (c) of Fig. 4 quantify the absolute and relative errors on the $\langle uv\rangle$ stress distribution compared to the DNS data[15] with and without the noncommutation procedure. It appears that, when the universal condition I is employed, the treatment recovers the commutation error beyond $y^+\sim 20$, where the recovery maintains values between 60% to 90% [Fig. 4(b)]. When condition II (which is suitable for specifing/imposing the evolution of the stresses along the wall) is used, a high error recovery (nearly 80%) is reached in the central part of the channel. Recovery values of the order of 50% are obtained around $y^+\sim 20$–30. It can be noticed that both the cases of the simulations based on the use of conditions I or II yield results that are in between the DNS and the experimental results. For example, the distance, measured through the norm L_2 in the interval $y^+\in[5,100]$, between the DNS and the experimental findings by Wei and Willmarth[18] is 18%, while the distance between the DNS and the present large-scale simulation (condition I) is only 4%. The situation described in Fig. 5 ($\mathrm{Re}_\tau=590$, reference DNS data base by Moser *et al.*[14]) is similar. Condition II performs better at $\mathrm{Re}_\tau=590$, where the accuracy is 3.5%, while the 7.3% is obtained at $\mathrm{Re}_\tau=180$.

The resolvable turbulence intensities are plotted in Figs. 6(a) and 6(b). Local discrepancies of the order of 10% (maximum) are observed with respect to the filtered DNS distributions, which is a good result and is somewhat better than the result offered by resolved simulations based on the

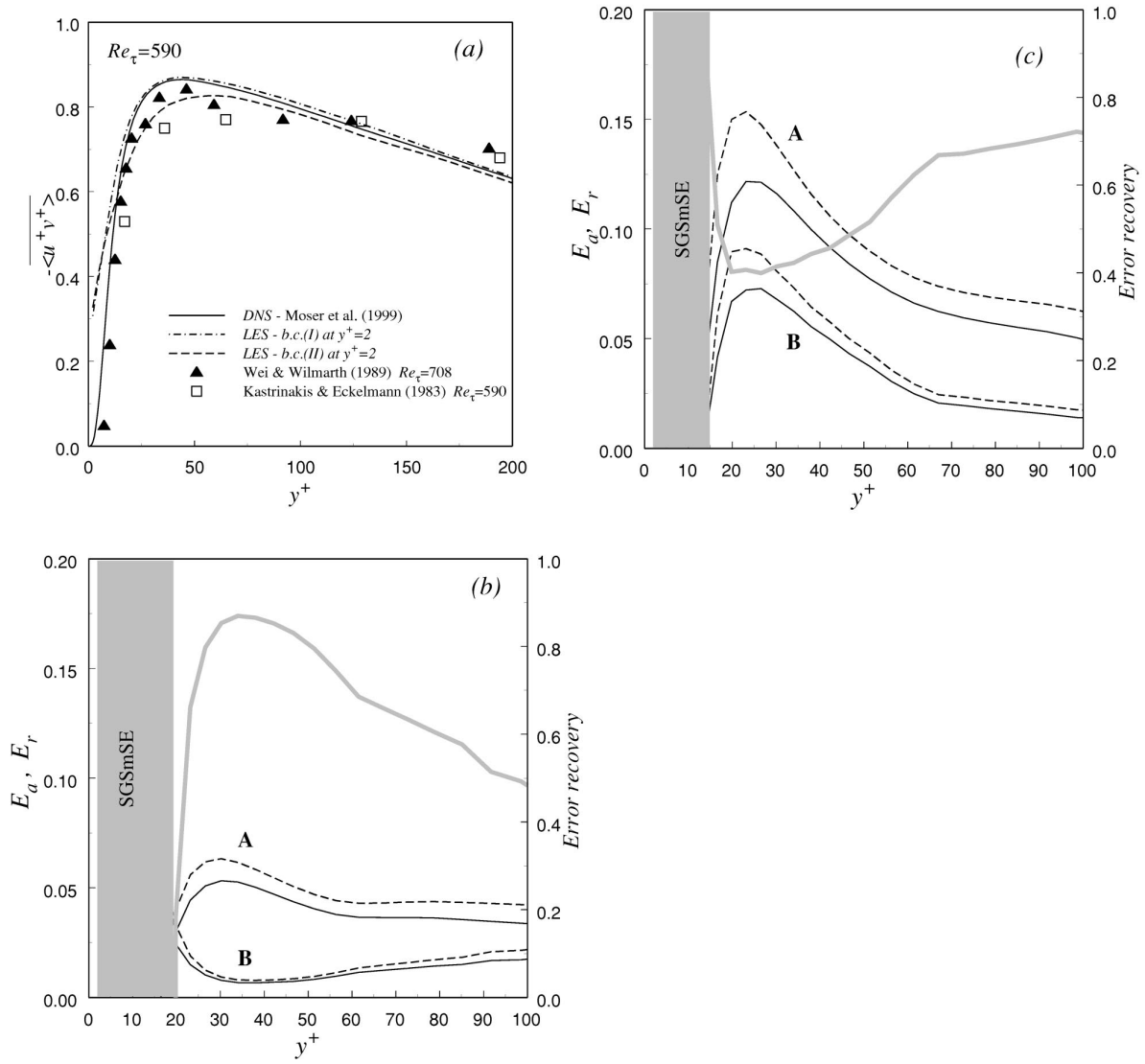

FIG. 5. Re_τ=590, Reynolds stress distribution across the channel. Absolute $E_a=\langle u^+v^+\rangle-\langle u^+v^+\rangle_{DNS}$ (—) and relative $E_r=[\langle u^+v^+\rangle-\langle u^+v^+\rangle_{DNS}/\langle u^+v^+\rangle_{DNS}]$ ×(----) error distributions on the Reynolds stress distributions for boundary conditions I (b) and II (c)—**A**, without the commutation correction, **B**, with the commutation correction. Gray continuous curve: error recovery $[E_a(\mathbf{A})-E_a(\mathbf{B})]/E_a(\mathbf{A})$. Shaded area: unreliable error distributions due to the systematic error of the SGS model.

dynamic Smagorinsky model. For example, in Ref. 19 local discrepancies of 15% can be observed. Always with regard to this set of data, the present simulation (condition I) shows an improvement, for the longitudinal turbulence intensity, of the accuracy with respect to the DNS data that decreases from 21.6% to 8%—the accuracy being based on the L_2 norm computed in the interval $2<y^+<50$. Instead, for the other turbulence intensity components, the accuracy is the same.

Figure 7 shows the ratio of the mean turbulent kinetic energy production to the mean dissipation due to molecular and eddy viscosity compared to the ratio relevant to the direct numerical simulations at Re_τ=180 and 590. In the present large-eddy simulations, due to the problem of SGSmSE (see Sec. IV), the dissipation function and the SGS stress are overestimated close to the wall. This explains not only the 5%, at Re_τ=180, and 15%, at Re_τ=590, reduction of the value of the peak but also the 70% difference in the position of the peak itself, which is located at $y^+\approx 20$. The ratio P/ε should in fact correctly peak at $y^+\approx 12$–13, which is, however, inside the layer of the unreliable results due to SGSmSE. This explains the inaccuracy in the peak position of the present simulations.

IV. CONCLUDING REMARKS

Wall conditions shifted from and laid parallel to the physical boundary of the flow domain have been presented. In this work we propose to use them together with the non-commutation explicit procedure to expound a new wall treatment for the resolved large-scale simulation of turbulent

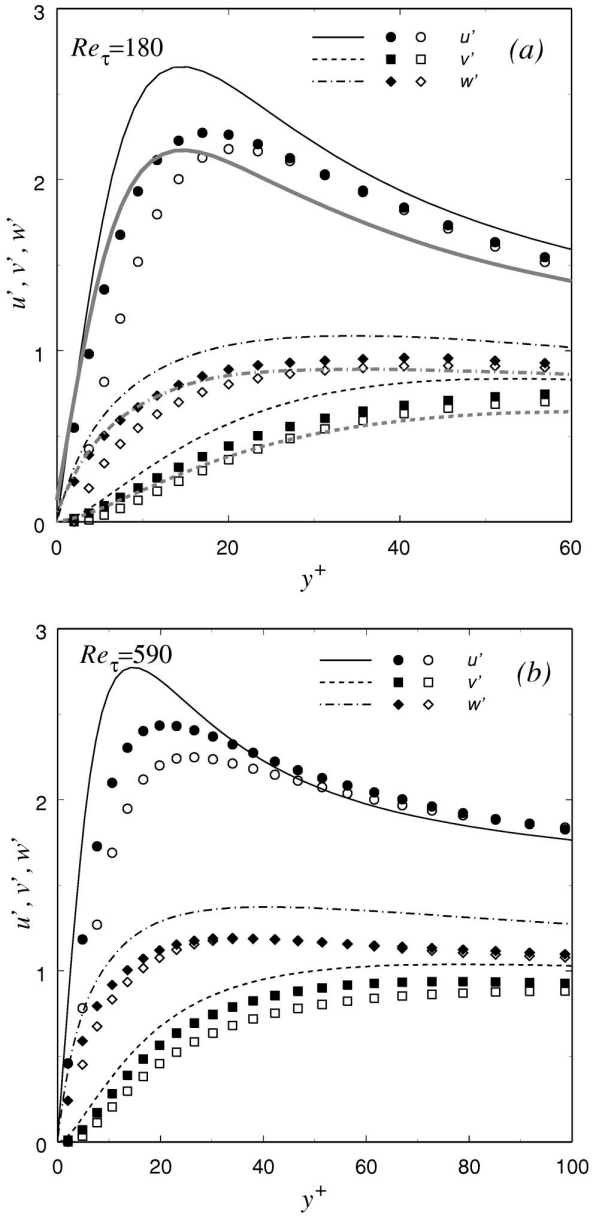

FIG. 6. Resolvable turbulence intensities, comparison with direct simulations. $u'=\sqrt{\overline{(\langle u\rangle-U)^2}}$, $v'=\sqrt{\overline{\langle v\rangle^2}}$, $w'=\sqrt{\overline{\langle w\rangle^2}}$. (a) $\mathrm{Re}_\tau=180$, DNS database by Passoni *et al.*; thin lines, unfiltered DNS; thick lines, filtered DNS. (b) $\mathrm{Re}_\tau=590$, DNS database by Moser *et al.*, only unfiltered data available. Symbols present LES, filled symbols bc I, and empty symbols bc II.

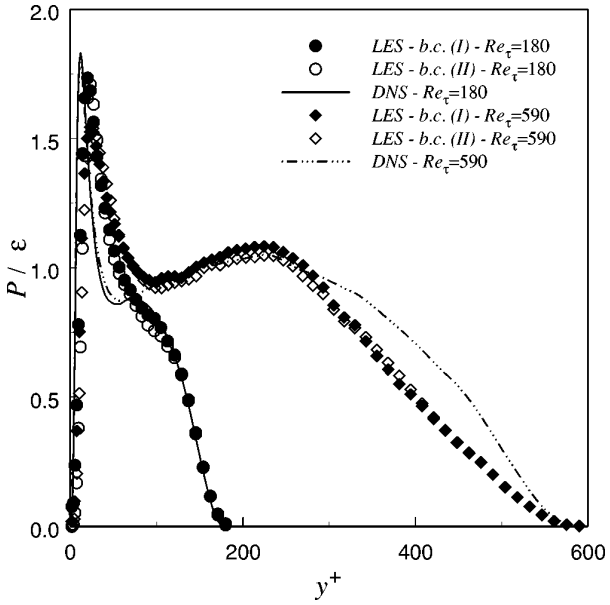

FIG. 7. Distribution of the mean energy production and dissipation ratio across the channel.

near-wall flows. The treatment was conceived to enhance, regardless of the SGS model performance, the large-eddy method applied to the resolved simulation of wall flows. For this reason, and also to test the capability of the treatment in detail, the SGS model employed in the large-eddy scale simulations was, deliberately, selected as it is the least appropriate eddy viscosity model for the near-wall region of the turbulent channel flow.

Two different wall conditions were obtained by combining approximate deconvolutions of the filtered velocities at the shifted boundary with a Taylor or a Mac Laurin series expansion of the unfiltered wall quantities. In this way a universal wall condition (Taylor's expansion, bc I) can be expressed at distances of about one viscous length from the wall, together with another condition that exploits the knowledge of the wall stress distribution and variation (Mac Laurins's expansion, bc II). This exploitation is a tool which can be useful to solve the inverse problem and whenever the wall stress (as well as, possibly, the heat wall flux) distribution and evolution are *a priori* known.

In general, despite the rather inappropriate SGS model that was deliberately used to test the capability of this near-wall treatment (see the analysis rationale in Sec. IV, the model used is the Smagorinsky model with a constant coefficient, as far as the comparison of model performances in LES is concerned; see, for instance, the case of the mixing layer presented in Meneveau and Katz[28]), the agreement between the present large-scale simulations, the DNS data, and the experimental observations is good, which confirms that coupling the explicit treatment of the noncommutation errors to one of the proposed two different kinds of no-slip and impermeability boundary conditions for the resolved variables is rewarding.

The noncommutation terms in the governing equations are important mainly in the near-wall part of the flow due to the filter gradient dependence. However, it has been confirmed that the noncommutation errors in the solution are also transferred toward the central part of the flow.[1] The relative errors in the central flow region, where the filter gradient is zero, are in fact lower but of the same order of magnitude as the local maximum error of the field. It can be noticed that the present wall treatment is able to substantially reduce not only the noncommutation errors but also the systematic error associated to the employment of the least appropriate SGS model. The accuracy given by the present

large-scale simulation is in general analogous to that given by simulation based on the adoption of the dynamic Smagorinsky model. However, it is better as far as the resolved longitudinal turbulent intensity is concerned.

Another property that should be highlighted is that, in the Reynolds number range of this investigation, the present near-wall treatment is able to show the same Reynolds number effects on the structure of the turbulent channel flow as those that are shown by laser-Doppler anemometer measurements.[18]

It can also be noticed that model condition II can transfer the structure of the wall-stress distributions to the flow without overconstraining the flow itself, because this is achieved formally through the imposition of only one condition, which is actually a velocity condition.

The present near-wall treatment is not proposed as an alternative to the use of the dynamic procedure. Rather, in the context of method improvements for large-eddy simulation, it is a preliminary operation to be followed by the optimization of the wall turbulence SGS model.

[1]M. Iovieno and D. Tordella, "Variable scale filtered Navier–Stokes equations: A new procedure to deal with the associated commutation error," Phys. Fluids **15**, 1926 (2003).
[2]S. Ghosal and P. Moin, "The basic equations for large eddy simulation of turbulent flows in complex geometries," J. Comput. Phys. **118**, 24 (1995).
[3]H. Van der Ven, "A family of large eddy simulation (LES) filters with non uniform filter widths," Phys. Fluids **7**, 1171 (1995).
[4]C. Fureby and G. Tabor, "Mathematical and physical constraints on large-eddy simulations," Theor. Comput. Fluid Dyn. **9**, 85 (1997).
[5]O. V. Vasilyev, T. S. Lund, and P. Moin, "A general class of commutative filters for LES in complex geometries," J. Comput. Phys. **146**, 82 (1998).
[6]U. Piomelli and E. Balaras, "Wall-layer models for large-eddy simulations," Annu. Rev. Fluid Mech. **34**, 349 (2002).
[7]J. W. Deardorff, "A numerical study of three-dimensional turbulent channel flow at large Reynolds numbers," J. Fluid Mech. **41**, 435 (1970).
[8]U. Schumann, "Subgrid scale model for finite difference simulations of turbulent flows in plane channels and anuli," J. Comput. Phys. **18**, 376 (1975).
[9]U. Piomelli, J. Ferziger, P. Moin, and J. Kim, "New approximate boundary conditions for large eddy simulations of wall-bounded flows," Phys. Fluids A **1**, 1061 (1989).
[10]E. Balaras, C. Benocci, and U. Piomelli, "Two-layer approximate boundary conditions for large-eddy simulations," AIAA J. **34**, 1111 (1996).
[11]J. S. Baggett, "On the feasibility of merging LES with RANS in the near-wall region of attached turbulent flows," *Annual Research Briefs* (Stanford University, Stanford, 1998), pp. 267–277.
[12]N. V. Nikitin, F. Nicoud, B. Wasistho, K. D. Squires, and P. R. Spalart, "An approach to wall modeling in large-eddy simulations," Phys. Fluids **12**, 1629 (2000).
[13]M. Iovieno, G. Passoni, and D. Tordella, "New approximate boundary conditions for the large eddy simulation of turbulent wall flows," 5th Euromech Fluid Mechanics Conference, Toulouse, 23–28 August 2003.
[14]R. D. Moser, J. Kim, and N. N. Mansour, "Direct numerical simulation of turbulent channel flow up to Re_τ=590," Phys. Fluids **11**, 943 (1999).
[15]G. Passoni, G. Alfonsi, and M. Galbiati, "Analysis of hybrid algorithms for the Navier–Stokes equations with respect to hydrodynamic stability theory," Int. J. Numer. Methods Fluids **38**, 1069 (2002).
[16]H. Eckelmann, "The structure of the viscous sublayer and the adjacent wall region in a turbulent channel flow," J. Fluid Mech. **65**, 439 (1974).
[17]E. G. Kastrinakis and H. Eckelmann, "Measurement of streamwise vorticity fluctuations in a turbulent channel flow," J. Fluid Mech. **137**, 165 (1983).
[18]T. Wei and W. W. Willmarth, "Reynolds-number effects on the structure of a turbulent channel flow," J. Fluid Mech. **204**, 57 (1989).
[19]M. Germano, U. Piomelli, P. Moin, and W. H. Cabot, "A dynamic subgrid-scale eddy viscosity model," Phys. Fluids A **3**, 1760 (1991).
[20]M. Germano, "Turbulence, the filtering approach," J. Fluid Mech. **236**, 325 (1992).
[21]R. H. Kraichnan, "Eddy viscosity in two and three dimensions," J. Atmos. Sci. **33**, 1521 (1976).
[22]A. Yoshizawa, "A statistically-derived subgrid model for the large-eddy simulation of turbulence," Phys. Fluids **25**, 1532 (1982).
[23]D. Carati and W. Cabot, "Anisotropic eddy viscosity models," in *Proceeding of the Summer Program* (Center for Turbulence Research, Stanford, 1996), pp. 249–259.
[24]M. Iovieno and D. Tordella, "The angular momentum equation for a finite element of fluid: A new representation and application to turbulent flows," Phys. Fluids **14**, 2673 (2002).
[25]H. O. Kreiss, "Difference approximation for boundary and eigenvalue problems for ordinary differential equations," Math. Comput. **26**, 605 (1972).
[26]J. Jimenez and P. Moin, "The minimal flow unit in near-wall turbulence," J. Fluid Mech. **225**, 213 (1991).
[27]P. Moin and J. Kim, "Numerical investigation of turbulent channel flow," J. Fluid Mech. **118**, 341 (1982).
[28]C. Meneveau and J. Katz, "Scale-invariance and turbulence models for large-eddy simulation," Annu. Rev. Fluid Mech. **32**, 1 (2000).